Scanning tunneling spectroscopy of a two-dimensional electron gas on the surface of ZnO

M. Wolovelsky, Y. Goldstein, and O. Millo*
Racah Institute of Physics, The Hebrew University, Jerusalem 91904, Israel
(Received 1 July 1997; revised manuscript received 8 September 1997)

Scanning tunneling microscopy and spectroscopy are employed in studies of ZnO single crystals. In particular we focus on spatially resolved tunneling spectroscopy of electron accumulation layers, produced by low-energy implantation of hydrogen ions on the oxygen $(000\bar{1})$ face. These layers constitute a quantized two-dimensional electron gas system on the *free* surface. The tunneling current-voltage (I-V) and dI/dV vs V curves acquired after implantation show structures which reflect the energy minima of the two-dimensional electronic subbands and localized surface states. [S0163-1829(98)01111-4]

In accumulation or inversion layers at a semiconductor surface, the associated electric field may be strong enough so that electrons are constrained to move parallel to the surface in a narrow potential well, and their motion perpendicular to the surface is quantized. Due to this confinement, the three dimensional conduction band splits up into a series of two-dimensional subbands, corresponding to the different eigenstates of the potential well. Each subband contains a continuum of levels, since the electrons are free to move parallel to the surface, and its energy minimum coincides with the energy of the corresponding quantized level.[1] Such two-dimensional electron gas (2DEG) systems have been subject to intensive research for quite a while now, mainly in metal-oxide-semiconductor structures and in the GaAs/Al_xGa_{1-x}As interface. The 2DEG in the systems above is embedded relatively deep in the sample, more than 100 nm away from the free surface, and is therefore not accessible to investigations via scanning tunneling microscopy (STM) and spectroscopy. Recently, STM studies were reported for the InAs(110) surface, where some of the data indicate an existence of quantized surface states.[2] The clean InAs(110) surface *cannot* inherently sustain a 2DEG. However, due to tip-surface interaction and Fermi-level pinning at step edges, strong accumulation layers may be formed by applied electric fields, resulting in quantized electron levels at the surface. Quantized accumulation layers at InAs-oxide interfaces have also been previously studied using *large-area* tunnel junctions.[3] In this paper we present localized tunneling spectroscopy measurements on a *self-sustained* 2DEG system produced at the *free* surface of ZnO by low energy implantation of H ions. A schematic energy diagram of the tip-sample tunnel junction after implantation is presented in Fig. 1. Our data clearly depict quantized electronic states in the 2DEG, and conform with theoretical calculations performed for this system.[4]

It has been demonstrated by our group, as well as by others, that the ‘‘oxygen’’ $(000\bar{1})$ face of ZnO can support extremely strong electron accumulation layers. Surface electron densities up to 2×10^{14} cm^{-2} have been achieved,[4–9] more than an order of magnitude higher than attained in the other systems described above. Such accumulation layers are characterized by a width of ~10 Å and nearly metallic volume concentration, and thus constitute a nearly perfect 2DEG system. A number of methods are available for producing these accumulation layers in ultra-high-vacuum conditions. Most effective, for our purpose, is via low-energy (100 to 400 eV) hydrogen-ion implantation resulting in a layer which is not sensitive to oxygen exposure (in contrast to all other methods).[5]

A variety of experiments have been carried out on ZnO accumulation layers, such as electrical transport and surface-capacitance measurements that established experimentally the two-dimensional nature of this electron system.[4–8] Low-energy electron loss spectroscopy has also been used, for studies of two-dimensional plasmons.[9] The latter technique, which is purely surface sensitive, was effective by virtue of the electron-rich layer located at the free surface. On the other hand, STM measurements on these accumulation layers, which may yield *direct* information on their quantized nature, have not yet been reported. Previous STM studies of ZnO were performed mainly on polycrystalline samples, demonstrating that the applicability of this technique can be extended to the regime of large band-gap semiconductors.[10,11] The spatially resolved tunneling current-voltage (I-V) characteristics manifested variations in the local electronic properties, correlated with morphological features such as grain boundaries. In particular, the authors studied the effect of adsorbates on the surface electronic properties due to induced band bending. However, quantized accumulation layers, as created and studied in our experiments, were not investigated in their work.

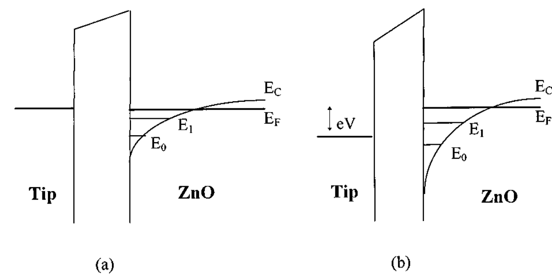

FIG. 1. Schematic energy diagram (drawn not to scale) of the tunnel junction between the STM tip and the ZnO surface after hydrogen implantation, with no applied tip-sample voltage (a) and with a positive tip voltage (b). In (a), the surface bending of the bottom of the conduction band, E_c is primarily due to the implantation. A narrow (~10–20 Å wide) potential well is created, confining electrons to the surface in a quantized accumulation layer; E_0 and E_1 represent minima of two-dimensional subbands. When positively biasing the tip, the band bending may increase, resulting in a narrower and deeper surface potential well (b). Consequently, the subband minima shift relative to each other and to higher energies with respect to the bottom of the potential well.

 © 1998 The American Physical Society

The ZnO single crystals were supplied by the Airtron Co. We have used samples having relatively high bulk conductivity, above 10^{-1} $(\Omega\ \mathrm{cm})^{-1}$ at room temperature. Such high conductivity is due to stoichiometric deficiency of oxygen,[12] resulting in a heavily n-doped, nearly degenerate semiconductor, where the Fermi level (E_F) is positioned within 100 meV from the bottom of the conduction band (E_C) in the bulk. The conductivity can be reduced to the intrinsic value, lower than 10^{-7} $(\Omega\ \mathrm{cm})^{-1}$, by annealing in oxygen atmosphere.[5] Low conductivity samples were used in the previous surface-transport measurements, in order to minimize the parallel bulk conductance and simplify the assessment of the 2DEG properties. These samples, however, are obviously hard to reliably measure with STM, therefore high conductivity samples were used in our research. Nevertheless, the contrast between tunneling spectroscopy measurements performed before and after hydrogen implantation is still clearly evident, as shown below.

The samples were cut to typical dimensions of $10\times5\times1\ \mathrm{mm}^3$ with the hexagonal C axis perpendicular to the large surface. The measurements were carried out on the oxygen $(000\bar{1})$ face of the crystal. The surface was polished with diamond lapping compound to a corrugation less than 1 μm, then etched for 30 sec in HCl and finally chemically polished in a 2% bromine methanol solution.

Our home-made STM is housed in a vacuum chamber having a base pressure of 1×10^{-9} Torr. The sample surface was cleaned by repeated cycles of 2 keV Ar-ion bombardment at a pressure of 5×10^{-5} Torr and subsequent annealing at 400–500 °C. The accumulation layers were produced *in situ* after the cleaning by implanting 200 eV hydrogen ions in the sample. The ionic penetration depth is less than 20 Å, thus the implanted ions reside very close to the surface. Consequently, a high electrostatic field is created, giving rise to a strong surface accumulation layer confined to the surface by a narrow potential well. The STM measurements were performed at different stages of surface preparation: after Ar ion milling, after annealing and after H implantation. We have acquired simultaneously topographic images and local I-V characteristics. The latter yield information on the local density of states, in particular on the two-dimensional (extended) and localized electronic surface states. The I-V curves were taken while momentarily disabling the feedback and scan circuits, and thus at constant tip-sample distance and lateral tip position.

Topographic images of the oxygen face of ZnO at different stages of surface preparation are shown in Fig. 2. The images were taken with a tip bias of -1 V and tunneling current of 0.6 nA. The size of the image presented in Fig. 2(a) is $40\times40\ \mathrm{nm}^2$, and was acquired after Ar ion milling and before any annealing process. One can see that the surface is disordered, and exhibits roughness having a lateral scale in the range of 1 to 10 nm. This roughness is due to both the polishing procedure, which obviously does not yield atomically flat surfaces, and to the Ar ion bombardment, which is expected to induce surface damage at the nanometer scale. Figure 2(b) depicts a square of side 400 nm after annealing. The average lateral roughness scale is now much larger, of the order of 100 nm and more, and the surface-roughness features such as shown in Fig. 2(a) (on the 1–10 nm range) have nearly completely vanished. Figure 2(c), of side 400 nm, was acquired after H implantation at an energy of 200 eV. It is clear, from comparing Figs. 2(b) and 2(c), that the H implantation does not damage the surface considerably. Similar to the previous works on ZnO,[10,11] we too did not yet achieve atomic resolution.

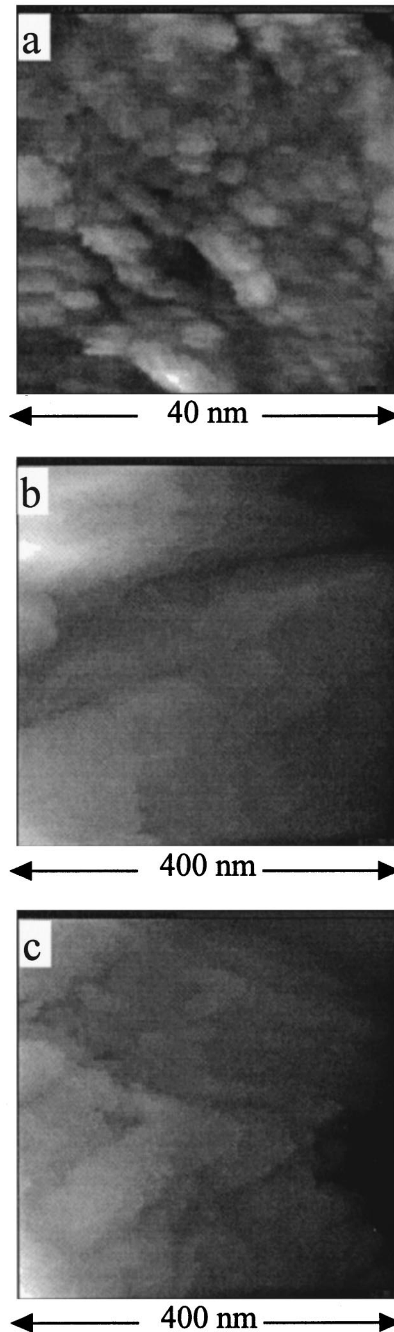

FIG. 2. Three STM topographic images of the oxygen surface of ZnO taken before annealing (a), after annealing (b), and after hydrogen implantation (c). The areas of the images are $40\times40\ \mathrm{nm}^2$, $400\times400\ \mathrm{nm}^2$, and $400\times400\ \mathrm{nm}^2$, respectively.

In Fig. 3 we present two tunneling I-V characteristics, one taken before H implantation (but after annealing) and the other after implantation, as denoted. Both were taken with the same setting of the tip bias and tunneling current (before disabling the feedback), -1 V and 0.25 nA, respectively. (Note that for positive voltage electrons flow from the sample to the tip, thus ZnO filled states are shown at positive bias.) The effect of implantation is clearly manifested by the difference between the two curves. First, the differential con-

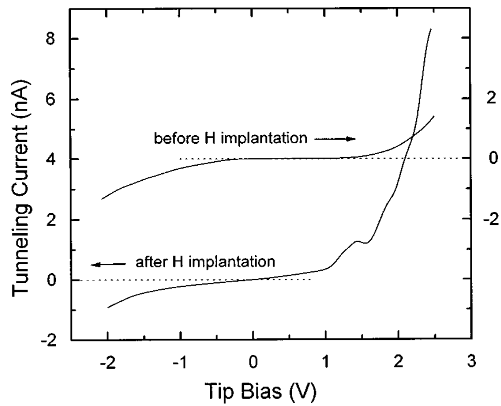

FIG. 3. Two tunneling I-V characteristics taken at room temperature on the oxygen surface of ZnO. The upper curve was acquired before hydrogen implantation and the lower curve after implantation, as denoted.

ductance (dI/dV) at zero bias is much larger after implantation. This results from the formation of a strong electron accumulation layer at the surface. Consequently, the surface electron density of states around E_F that are available for tunneling is enhanced. More significant is the difference between the two curves at bias voltages larger than ~ 1 V. The curve taken before implantation keeps growing *smoothly* and exhibits no significant structure. Its parabolic shape results mainly from the monotonic increase of the tunneling rate with applied voltage due to reduction of the average tunnel-barrier height.[13,14] The curve taken after implantation shows, on the other hand, a much richer structure at this voltage range. One can observe a peak manifesting negative differential resistance (NDR) at 1.4 V tip bias and a faint step structure (which is well resolved in the derivative traces presented in Fig. 4) at larger bias. We attribute the NDR to tunneling through localized surface states (similar to Ref. 15) and the structure at larger bias to the two-dimensional subbands (of extended states), as explained below. Note that the H implantation does not affect much the I-V curve at large negative voltages. In this voltage range electrons tunnel from the tip to available empty states above the ZnO Fermi energy, and on both sides of the tunnel junction the electronic density of states is a smooth, structureless, function of energy.

We note that our I-V curves do not exhibit a large energy band gap ~ 3.2 eV, characteristic of ZnO,[5,12] namely, we do not observe a plateau in the I-V curves. This is because we performed our measurements on *conducting*, heavily doped samples, as noted above. Furthermore, positive tip-bias enhances the ZnO surface electron concentration, reduces the tunnel-barrier height, and consequently the tunneling conductance is increased. In fact, our I-V curves taken *before implantation* are similar to some of those presented in Refs. 10 and 11, obtained for samples having similar transport properties to ours. The authors of those papers accounted for their data assuming that there is a weak depletion layer on the surface and that the Fermi level is not pinned. This may also be the case in our samples before implantation, although we do not have enough data to uniquely establish these conjectures.

The surface states are manifested more clearly in the differential tunneling conductance, dI/dV vs V, traces presented in Fig. 4, where we focus, according to the discussion above, only on the positive bias range. (Curves are shifted vertically, for clarity.) The lower curve was acquired before implantation, and it is indeed smooth and structureless. The increase with applied bias of the differential tunneling conductance is primarily due to the reduction of the average barrier height, as noted above. The upper three curves were taken after implantation, at different lateral tip positions over the sample. These three curves, as well as *all* dI/dV characteristics measured after implantation, exhibit a series of three *major* peaks, which are not always well resolved (e.g., the middle peak in the second curve from the top appears more similar to a shoulder). The dI/dV curves are time independent for a given tip position (at least for time scales of the order of one hour). The *exact* positions of the peaks vary from one tip position to another, due to surface inhomogeneity which should be prominent in the disordered surface obtained after implantation. The general features, however, are reproducible, as evident from the figure. The first peak of each curve, labeled ''localized'' at the upper curve, corresponds to the NDR peak in Fig. 3 and is attributed to tunneling through a localized surface state. The two peaks at larger voltages reflect, we believe, the minima of the first and second subbands, and are accordingly labeled E_0 and E_1, respectively (using the notation of Fig. 1 and Ref. 4).

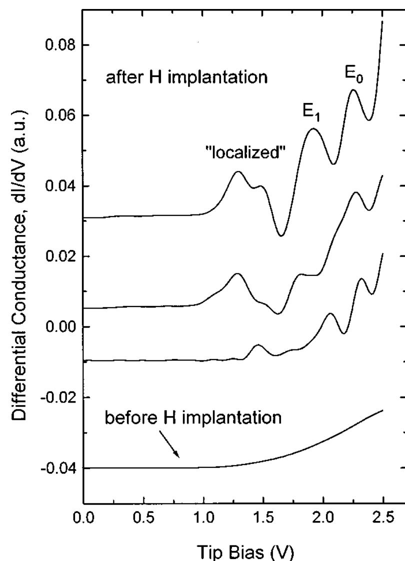

FIG. 4. Differential conductance dI/dV vs V curves taken on the oxygen face of ZnO. The lower curve was acquired before hydrogen implantation. The three upper curves were measured after implantation, at different lateral tip positions. The peaks labeled E_0 and E_1 reflect the minima of two-dimensional subbands at the specific tip position, and the peak labeled ''localized'' is due to tunneling through a localized surface state, see text.

We shall first discuss the large bias region of the I-V curves, where the characteristics resemble those acquired on the 2DEG at the InAs-oxide interface (see Ref. 3), and come back later to the NDR feature. The shape of the curves, in particular the occurrence of the two peaks (E_0 and E_1), needs some explanation. As E_F of the tip sweeps down across a subband minimum [e.g., E_1 in Fig. 1(b)], one expects to observe a sharp *drop* in the differential tunneling conductance due to a sharp decrease in the density of ZnO surface-

electron states at energy equal to E_F of the tip. (Recall that the electronic density of states for each two-dimensional subband is constant, independent of energy.) This contribution to the conductance variation is superimposed on another, which tends to *increase* the differential tunneling conductance, namely, the reduction in the average barrier height upon raising the bias. The result of the above two opposing contributions is a dI/dV vs V curve exhibiting peaks superimposed on an otherwise monotonically increasing line; each peak appears approximately at an energy where the Fermi level in the tip crosses the minimum of a two-dimensional subband at the specific tip location.

The positions of the peaks in the dI/dV vs V curves relative to each other do not exactly yield the energies of the subband minima. The reason is, that part of the voltage applied between the tip and the sample drops in the accumulation layer, so as the bias voltage is increased, the surface band bending also increases, and the energy minima consequently shift, as illustrated in Fig. 1. However, this process has only a small effect in our case, since, due to the strong initial accumulation layer (after implantation), the Fermi level at the ZnO surface is effectively pinned. This is because a very large amount of additional charge is now required to significantly affect the space charge region. Indeed, we do find that the difference between the measured peak positions agree fairly well, to within 0.1 eV, with the theoretical prediction[4] for a surface electron density of 5×10^{13} cm^{-2}, a reasonable value in our case. At this concentration only two subbands are predicted to be below E_F, and the energy minima difference E_1-E_0 is $\sim$0.4 eV.[4] This is one reason, in addition to its shape, that we relate the NDR peak to localized surface states.

We would like to note here that in *our* case, the tunneling probability is not very sensitive by itself to the wave-vector component parallel to the surface, since the penetration depth of the 2DEG (''envelope'') wave functions into the vacuum is constant for a given subband, independent of the parallel wave vector.[4] (There is, of course, an indirect dependence due to the fact that tunneling into or from higher energy levels takes place at larger bias and thus with reduced barrier height, as noted above.) Moreover, the conservation rule of parallel wave vector is not strictly obeyed, due to surface disorder. Thus, it is nearly impossible to determine the subband dispersion relation from our I-V traces. This is in contrast to the case of three-dimensional electron states and ordered surfaces discussed in Refs. 13 and 14. We also could not employ the method introduced by Hasegawa and Avouris[16] and by Crommie *et al.*,[17] who determined the dispersion relation of two-dimensional states at Au(111) and Cu(111) surfaces, respectively. The relatively rough ZnO surface makes it impossible to image standing-wave patterns in the local density of states formed by interference of the two-dimensional surface states. However, our transport measurements[6] indicate that despite the relatively large surface disorder, the electronic wave-functions are *extended* and the system is in the *metallic* diffusive weakly localized transport regime.[18] The NDR peak shown in Fig. 3 (and the corresponding structure in Fig. 4) are similar to previous observations of tunneling through surface localized states, e.g., by Lyo and Avouris for submonolayer boron covered Si(111) surface.[15] These authors have shown that at *specific* tip locations the I-V curves exhibit NDR, attributed to tunneling through localized atomiclike states. We think that also our characteristics manifest tunneling through localized states, which are probably induced by the implantation process. In our case, however, NDR is observed at *every* tip position, although it is not always very pronounced. This is due to the high spatial density of induced localized states that may constitute, in effect, a two-dimensional surface impurity band.

In summary, self-sustained quantized electron accumulation layers at the free oxygen surface of ZnO were studied using scanning tunneling spectroscopy. The I-V and dI/dV vs V characteristics directly reflect a spectrum of surface states that consists of both localized levels and the minima of two-dimensional subbands of the 2DEG. These characteristics vary in a reproducible (time-independent) way with lateral tip position, manifesting spatial fluctuations of the local electronic and surface properties.

We thank Nira Shimoni and Yair Levi for helpful discussions and for their assistance in preparing this manuscript. This work was supported by the Israel Science Foundation Grant No. 032-7625.

*Author to whom correspondence should be addressed. FAX: +972-2-6584437. Electronic address: milode@vms.huji.ac.il

[1] T. Ando, A. B. Fowler, and F. Stern, Rev. Mod. Phys. **54**, 434 (1982).

[2] J. Wildöer, Ph.D. thesis, University of Nijmegen and Delft University of Technology, 1996.

[3] D. C. Tsui, Phys. Rev. B **4**, 4438 (1971).

[4] D. Eger and Y. Goldstein, Phys. Rev. B **19**, 1086 (1979).

[5] G. Yaron, A. Many, and Y. Goldstein, J. Appl. Phys. **58**, 3508 (1985).

[6] Y. Goldstein and Y. Grinshpan, Phys. Rev. Lett. **39**, 953 (1977); Y. Goldstein, Y. Grinshpan, and A. Many, Phys. Rev. B **19**, 2256 (1979); M. Nitzan, Y. Grinshpan, and Y. Goldstein, *ibid.* **19**, 4107 (1979).

[7] D. Kohl, H. Moormann, and G. Heiland, Surf. Sci. **73**, 160 (1978).

[8] E. Veuhoff and D. Kohl, J. Phys. C **14**, 2395 (1981).

[9] Y. Goldstein, A. Many, I. Wagner, and J. I. Gersten, Surf. Sci. **98**, 599 (1980); A. Many *et al.*, Phys. Rev. Lett. **46**, 1648 (1981).

[10] D. A. Bonnel and D. R. Clarke, J. Am. Ceram. Soc. **71**, 629 (1988).

[11] G. S. Rohrer and D. A. Bonnel, J. Vac. Sci. Technol. B **9**, 783 (1991).

[12] R. Littbarski, in *Zinc Oxide*, edited by W. Hirschwald *et al.*, Vol. 7 of *Current Topics in Materials Science*, edited by E. Kaldis, (North-Holland, Amsterdam, 1981), p. 212.

[13] see, e.g., E. L. Wolf, *Principles of Electron Tunneling Spectroscopy* (Oxford University Press, Oxford, 1989), Chap. 2.

[14] R. M. Feenstra, J. A. Stroscio, and A. P. Fein, Surf. Sci. **181**, 295 (1986).

[15] I.-W. Lyo and Ph. Avouris, Science **245**, 1369 (1989).

[16] Y. Hasegawa and Ph. Avouris, Phys. Rev. Lett. **71**, 1071 (1993).

[17] M. F. Crommie, C. P. Lutz, and D. M. Eigler, Nature (London) **363**, 524 (1993).

[18] G. Bergman, Phys. Rep. **107**, 1 (1984), and references therein.